J Physiol Sci (2011) 61:313–319
DOI 10.1007/s12576-011-0150-2

ORIGINAL PAPER

Comparison of protein behavior between wild-type and G601S hERG in living cells by fluorescence correlation spectroscopy

Eri H. Hayakawa · Michiko Furutani · Rumiko Matsuoka · Yuichi Takakuwa

Received: 6 January 2011 / Accepted: 17 April 2011 / Published online: 15 May 2011

Abstract The human ether-a-go-go-related gene (hERG) protein is a cardiac potassium channel. Mutations in hERG can result in reductions in membrane channel current, cardiac repolarization, prolongation of QT intervals, and lethal arrhythmia. In the last decade, it has been found that some mutants of hERG involved in long QT syndrome exhibit intracellular protein trafficking defects, while other mutants sort to the membrane but cannot form functional channels. Due to the close relationship between intracellular trafficking and functional protein expression, we aimed to measure differences in protein behavior/motion between wild-type and mutant hERG by directly analyzing the fluorescence fluctuations of green fluorescent protein-labeled proteins using fluorescence correlation spectroscopy (FCS). Our data imply that FCS can be applied as a new diagnostic tool to assess whether the defect in a particular mutant channel protein involves aberrant intracellular trafficking.

Keywords Intracellular protein transport · Cardiovascular research · Imaging · Arrhythmia · Potassium channels · Fluorescence correlation spectroscopy (FCS)

E. H. Hayakawa (✉) · M. Furutani · R. Matsuoka · Y. Takakuwa (✉)
International Research and Educational Institute for Integrated Medical Sciences (IREIIMS), Tokyo Women's Medical University, 8-1 Kawata-cho, Shinjuku-ku, Tokyo 162-8666, Japan
e-mail: erihayakawa@jichi.ac.jp

Y. Takakuwa
e-mail: takakuwa@research.twmu.ac.jp

M. Furutani · R. Matsuoka
Department of Pediatric Cardiology, Tokyo Women's Medical University, 8-1 Kawata-cho, Shinjuku-ku, Tokyo 162-8666, Japan

Y. Takakuwa
Department of Biochemistry, Tokyo Women's Medical University, 8-1 Kawata-cho, Shinjuku-ku, Tokyo 162-8666, Japan

Present Address:
E. H. Hayakawa
Laboratory of Medical Zoology and Parasitology, Department of Infection and Immunity, Jichi Medical University, 3311-1 Yakushiji, Shimotsuke, Tochigi 329-0498, Japan

Introduction

The human ether-a-go-go-related gene (hERG) protein is a cardiac potassium channel. Mutations in hERG can result in a reduction in channel current [1, 2], defective cardiac repolarization, a prolonged electrocardiac QT interval, and arrhythmia, which can lead to sudden death. Some mutants of hERG that cause long QT syndrome are associated with abnormal intracellular protein trafficking [3, 4]. In a previous study, we reported that G601S is an hERG mutant ($Gly^{601} \rightarrow Ser^{601}$) that is unable to form a functional channel in the plasma membrane, resulting in a reduction in total potassium currents [2]. G601S also has a smaller molecular weight (135 kDa) than the mature wild-type (WT) protein (155 kDa) because of its different glycosylation level. WT hERG can exist as 135-kDa and 155-kDa molecular forms [5], according to its two levels of glycosylation, which are often termed "core" and "full" glycosylation, respectively. G601S, in contrast, is subject to only core glycosylation [6], which may be responsible for the observed abnormal protein expression. Although the importance of glycosylation in protein expression and trafficking has been suggested [7, 8], the effect of glycosylation on the expression and function of WT hERG and G601S is not fully understood. Moreover, in

affected patients, G601S is co-expressed with the WT hERG form and behaves as a dominant negative. Because of this co-expression, the precise identification of G601S in the cell to study its expression, and trafficking is challenging. The most common analytical method used for studying channel proteins, including WT hERG and its mutants, is patch clamping [9, 10]. However, this is only suitable for channel proteins that are functional at the cell membrane. In contrast, studying "molecular motion" according to differences in molecular weight could allow us to differentiate G601S from WT hERG. To achieve this goal, a microscopy technique with high temporal and spatial resolution is required in combination with conventional biochemical assays.

There are several techniques for the measurement of single molecules that enable direct visualization of the behavior of proteins in live cells. These include fluorescence recovery after photobleaching (FRAP), fluorescence resonance energy transfer (FRET), single particle tracking (SPT), and fluorescence correlation spectroscopy (FCS). FRAP is suitable to measure the diffusion of molecules in a large area but has a relatively low temporal resolution. FRET is suitable for protein-protein interactions [11, 12] and protein distribution, but not for protein motion. SPT is suitable for measuring molecular motion in a small to large area; however, it can only assess a limited number of particles, and its resolution is highly dependent on the acquisition rate [13, 14]. The accuracy of SPT data also depends on the surface morphology of the observed cell. Tracking of target particles is often lost at the edge of the cell and when the paths of multiple particles cross over.

FCS, in contrast, detects fluorescence intensity fluctuations within a limited focal volume (approximately 1×10^{-15} l) and estimates molecular motion using a correlation analysis of the fluorescence signals (Fig. 1). The temporal resolution of FCS is much higher (microseconds) than that of any other fluorescence-based single particle technique. Since the fluorescence fluctuations of a particle are dependent on particle mass and concentration [15], the measured fluorescence signals can be converted to the diffusion rate of the particle. Therefore, changes in the diffusion rate of the targeted molecules reflect changes in the molecular mass because of interactions with secondary molecules, biochemical reactions, and enzymatic reactions [16, 17]. With these advantages, FCS has been used to study fast molecular biological events [18].

For the above reasons, FCS is suitable for studying and distinguishing the intracellular behaviors of the WT hERG and G601S proteins at the single particle level in living cells. Here, we tested a new method for evaluating protein function by investigating protein trafficking parameters. We also tested whether this method could predict whether the protein would be expressed and would function normally. To our knowledge, this is the first study of FCS applied to detect the behavior of proteins related to cardiac channelopathies.

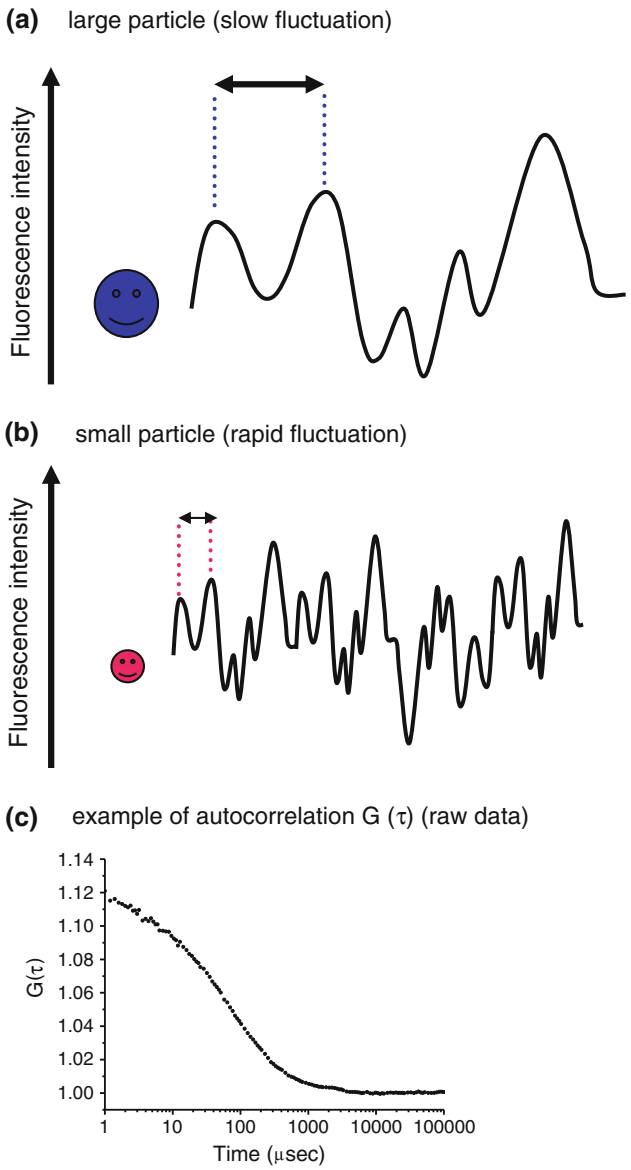

Fig. 1 FCS monitors the random motion of fluorescently labeled molecules. These fluctuations provide information on the diffusion time of a particle and are directly dependent on the molecular size. For a large molecule, the fluorescence fluctuation is slow (**a**), whereas a small molecule makes rapid fluctuations (**b**). Consequently, any increase in the mass of a molecule (for example, as the result of an interaction with a second molecule) is readily detected as an increase in the particle's diffusion time. An actual $G(\tau)$ plot curve of Rho6G is shown as an example (**c**)

Materials and methods

DNA constructs and transfection

We used human embryonic kidney 293 cells (HEK293; American Type Culture Collection No. CRL-1573) for our expression system. WT hERG or G601S mutant hERG was expressed in pcDNA3 [2]. Both plasmids expressed the

coding region of green fluorescent protein (GFP) at the amino terminus of the channel peptide. HEK293 cells were maintained in GIT (#398-00515; Nihon Seiyaku, Tokyo, Japan) with 10% fetal bovine serum and 2% penicillin-streptomycin (#15140148; Gibco, Carlsbad, CA). Transfection was performed by adding 0.5 μg of WT-hERG/pcDNA3 or G601S-hERG/pcDNA3 to cells with Effectene Transfection Reagent (#301425; Qiagen, Valencia, CA) according to the manufacturer's instructions. The medium was changed to Opti-MEM I Reduced-Serum Medium (#11058-021; Invitrogen, Carlsbad, CA) to reduce the background before FCS and imaging. Protein localization and protein diffusion rates were measured on days 1 and 2 after transfection.

Confocal light microscopy and FCS measurements

FCS was performed with a Zeiss LSM510 ConfoCor 2 confocal microscope (Carl Zeiss, Jena, Germany) with a 40× water immersion objective lens, numerical aperture (NA) = 1.2 (pinhole width, 70 μm) [19]. Fluorescence signals were observed using a 488-nm laser and a 505- to 550-nm band-pass emission filter. We set the observational spot from the cytosol to the cell membrane. FCS measurements and analysis were carried out as previously described [18, 20, 21].

Briefly, the fluorescence autocorrelation function $F(\tau)$ was fitted using the following equation:

$$\begin{aligned} F(\tau) &= \langle I(t)\rangle \cdot \langle I(t+\tau)\rangle \\ &= \langle (\sigma I(t) + \langle I\rangle)(\sigma I(t+\tau) + \langle I\rangle)\rangle \\ &= \langle (\sigma I(t) \cdot \sigma I(t+\tau)\rangle + \langle I\rangle^2 \end{aligned}$$

where $\langle I(t)\rangle$ is the average fluorescence intensity, t is time, $t + \tau$ is the intensity measured at a later time, and $\sigma I(t)$ and $\sigma I(t + \tau)$ are the deviation from the average fluorescence intensity.

The normalized fluorescence autocorrelation function $G(\tau)$ was defined as:

$$G(\tau) = 1 + \frac{\langle (\sigma I(t) \cdot \sigma I(t+\tau)\rangle}{\langle I\rangle^2}$$

The acquired $G(\tau)$ was fitted using a one- or two-component model as:

$$G(\tau) = \frac{1}{N}\sum_i F_i \left(1 + \frac{\tau}{\tau_i}\right)^{-1} \left(1 + \frac{\tau}{S^2\tau_i}\right)^{-1/2} + 1$$

where F_i and τ_i are the fraction and diffusion time of component i, respectively. N is the average number of fluorescently labeled particles in the excitation-detection volume of the laser beam [18].

We first measured the diffusion time of rhodamine 6G (Rho 6G) (1×10^{-7} M); τ_{Rho6G} was a standard value when the microscope was started up each time. The diffusion coefficient of Rho 6G; D_{Rho6G} (2.8×10^{-6} cm^2/s), was used as an authentic value. After the diffusion time of the WT hERG or G601S samples was measured (τ_{sample}), their diffusion coefficients (D_{sample}) were calculated using the equation:

$$D_{\text{sample}}/D_{\text{Rho6G}} = \tau_{\text{Rho6G}}/\tau_{\text{sample}}$$

The fluorescence fluctuation signal was monitored for 50 s and this was repeated six times to obtain the diffusion rate.

Results

In this study, we focused on determining whether FCS is able to identify differences in particle behavior between WT hERG and G601S in the cytosol, where both proteins are located individually. hERG is formed as a tetramer in cells. If wild-type hERG and mutant G601S hERG are co-transfected at the same time, there are five possible formations and we cannot control which subtypes are expressed. We also cannot investigate the causal relationships without determining the expressed protein's structure and function. Based on this reason, we transfected the wild-type and mutant protein into cells independently and measured their fluctuations and diffusion rates by FCS separately.

Figure 2 shows the localization of GFP-tagged WT and G601S hERG in HEK293 cells the day after transfection. Although WT is reported to localize at the plasma membrane, we observed WT hERG throughout the cytosol, up to and at the plasma membrane. This distribution indicates that some WT hERG molecules were being trafficked to the plasma membrane. In contrast, G601S was detected in the cytosol only; no membrane localization was observed.

On day 2, WT hERG was clearly accumulated at the plasma membrane as well as in the cytosol (Fig. 2c). However, G601S remained only in the cytosol, and there was an area where no protein localization was detected (arrowhead in Fig. 2d). These data show that the single mutation G601S in WT hERG had a dramatic effect on protein trafficking.

Next, we measured the molecular motion of WT hERG and G601S in the cytosol. On day 1, both forms showed two distinct diffusion patterns: a fast diffusion (D1) and a slow diffusion (D2) (Fig. 3). This suggests that both have at least two different molecular forms in living cells. The D1 value ($3.08 \times 10^{-8} \pm 1.72 \times 10^{-8}$ cm^2/s; mean ± SD) for WT hERG was approximately 100 times faster than the D2 value ($2.45 \times 10^{-10} \pm 9.93 \times 10^{-11}$ cm^2/s). For G601S, D1 ($8.54 \times 10^{-8} \pm 3.30 \times 10^{-8}$ cm^2/s) was approximately 200 times faster than D2 ($3.82 \times 10^{-10} \pm 2.02 \times 10^{-10}$ cm^2/s).

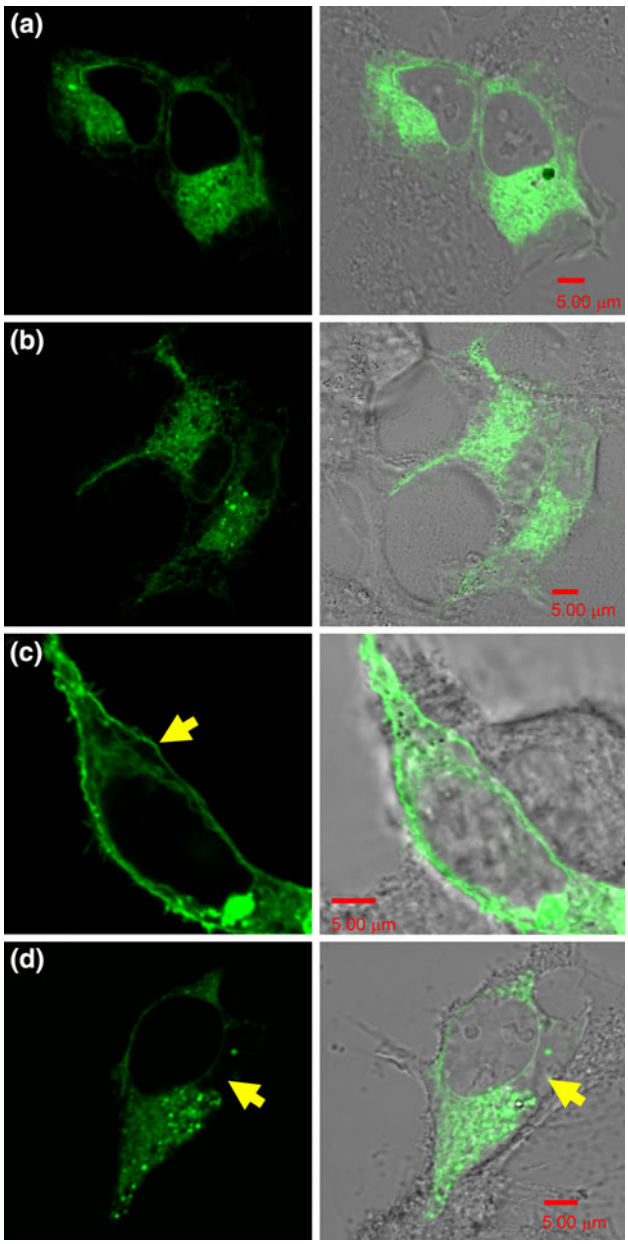

Fig. 2 The localization of GFP-tagged wild-type hERG (**a**) and G601S (**b**) the day after transfection of their respective expression constructs. The *left-hand panels* show confocal-imaged, GFP-labeled G601S and WT hERG channels in HEK293 cells. The *right-hand panels* show merged Nomarski images and GFP fluorescence images. At 24 h after transfection, the protein localizations of WT hERG and G601S are indistinguishable. On day 2, approximately 48 h after transfection, WT hERG (**c**) was localized at the plasma membrane more than in the cytosol (*arrow*). In contrast, G601S was not trafficked through the cytosol to the plasma membrane (**d**) (*arrow*). All *scale bars* are 5 μm

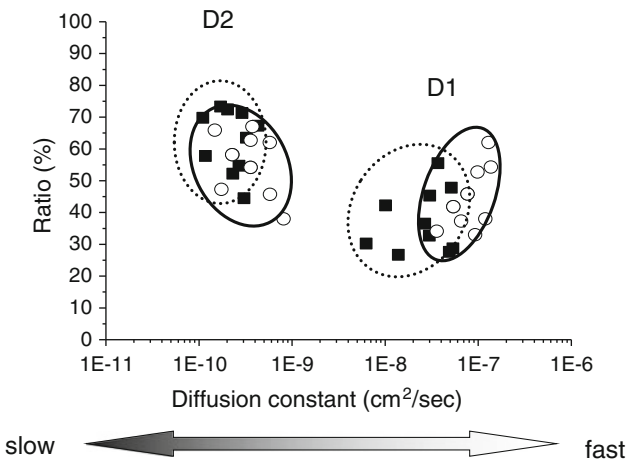

Fig. 3 Comparison of diffusion coefficients between wild-type hERG and G601S in the cytosol on day 1 by FCS measurements. Both proteins contained two components of the diffusion coefficient. There was a statistically significant difference in the fast, D1 component between WT hERG (*filled squares*, *dotted line circle*) and G601S (*unfilled circles*, *solid line circle*). However, the slow, D2 component motions were statistically indistinguishable between WT hERG and G601S

It should be noted that the average D1 for G601S was more than two-fold higher than that of the WT hERG D1 ($p = 1.62 \times 10^{-4}$ by *t* test). Incomplete glycosylation of G601S could be responsible for the increase in D1. However, there was no significant difference in D2 between WT hERG and G601S. It is not clear what D1 and D2 represent, but D1 may represent the free form of protein or vesicle movement, while D2 may represent the diffusion of proteins or vesicles in more restricted environments such as when associated with intracellular organelles [22]. These FCS data clearly showed that the high sensitivity and temporal resolution of FCS can reveal "multi-modal" protein diffusion within living cells.

The glycosylation patterns of mature WT hERG (core and full glycosylation) are essential for correct protein trafficking and function. To test whether the diffusion coefficient changes during the protein trafficking, we compared FCS data for WT hERG between the plasma membrane and cytosol regions (Fig. 4a, b). D1 at the plasma membrane ($2.65 \times 10^{-8} \pm 1.61 \times 10^{-8}$ cm^2/s) was not significantly different from that in the cytosol ($p = 0.55$) but was just a little slower ($3.08 \times 10^{-8} \pm 1.72 \times 10^{-8}$ cm^2/s). The D2 values were also indistinguishable between the two locations ($2.09 \times 10^{-10} \pm 1.19 \times 10^{-10}$ vs. $2.45 \times 10^{-10} \pm 0.99 \times 10^{-10}$ cm^2/s) ($p = 0.46$). However, in the cytosol, the proportions of the D1 and D2 components were 37.3 and 62.7%, respectively, whereas at the plasma membrane, the slow, D2 component was increased significantly to approximately 74.0%. These data show that the majority of newly expressed proteins were delivered as fully mature and functional forms of WT hERG to the plasma membrane.

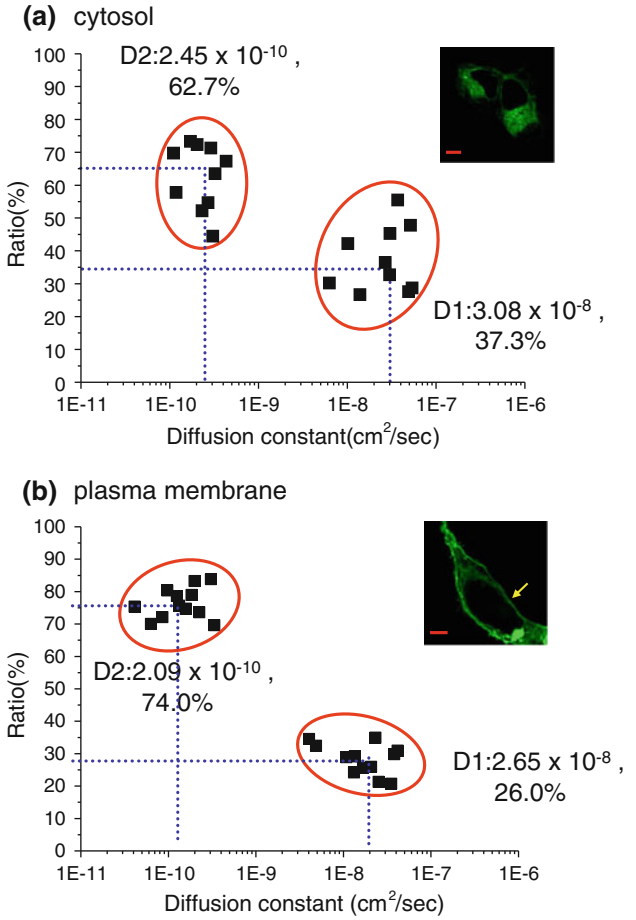

Fig. 4 Comparisons of the D1 and D2 diffusion coefficients for wild-type hERG on day 1 (**a**) and day 2 (**b**) after transfection. The proportion of slowly diffusing particles was greater on day 2 than on day 1 (*t* test; $p = 0.002$). In the fluorescence images, GFP-WT hERG clearly localized at the plasma membrane (*arrow*). All *scale bars* are 5 μm

Discussion

In this study, we showed that FCS could detect two separate protein populations with different diffusion coefficients, both at the plasma membrane and in the cytosol. It is likely that multiple factors are involved in determining the diffusion coefficient for each protein population between the plasma membrane and the cytosol. When proteins exist in the plasma membrane, the protein motion likely slows down within tightly packed areas such as rafts, which are rich in sphingomyelin and cholesterol. Fast motion at the membrane may suggest protein motion outside the raft. Other proteins in the same voltage-gated K^+-channel protein family, KCNA5 and KCNB1, have been suggested to exist in rafts and noncaveolae lipid raft regions [23, 24]. Furthermore, these proteins are six-transmembrane structures and their three-dimensional structures are very similar to that of hERG. Based on these data, hERG may preferentially exist in the lipid raft domains. Biophysical analyses of membrane protein diffusion using SPT have also revealed a complex protein diffusional motion [25–27]. Murase et al. [27] reported a "hop" diffusion of 1,2-dioleoyl-*sn*-glycero-3-phosphoethanolamine (DOPE) in HEK293 cells with a mean diffusion coefficient of approximately 4×10^{-9} cm^2/s. This value was based on analyses with lower temporal resolution than afforded by the SPT experiments, but yielded data similar to the mean of our two diffusion coefficients (10^{-8}–10^{-10} cm^2/s) at the plasma membrane. Furthermore, the proportion of slow components on day 2 became larger than that on day 1, indicating that more WT hERG had accumulated at the plasma membrane by day 2 (approximately 48 h after transfection).

In the cytosol, fast diffusional motion may reflect the protein moving freely during vesicle trafficking, whereas slow diffusional motion may originate from proteins associated with intracellular organelles such as the endoplasmic reticulum (ER) and Golgi. In the protein trafficking pathway, abnormally folded proteins are normally removed by the quality control systems of the ER and are subject to retrotranslocation and degradation. The localization of G601S (Fig. 2) and its failed form having been extracted from the trafficking pathways by the ER quality control systems could contribute to its fast D1 diffusion value.

Advantages and limitations of FCS

The abilities of imaging-based light microscopy for single molecules are always constrained by the light diffraction limit, the data acquisition rate, and the fluorescence intensity. In addition, techniques such as SPT are only successful with well-separated fluorescence spots to establish a "single molecule" condition; this requires special sample preparation techniques. All of these issues make single molecule observation in real time a highly difficult undertaking. However, FCS records fluorescence fluctuations within an extremely small volume at high acquisition rates, allowing a high sensitivity for dynamic molecular behaviors. A notable advantage of FCS is that no special sample preparation techniques are required. This is very convenient in biomedical research in situations where high expression of target proteins is difficult to attain or when only a small quantity of the sample can be observed. FCS is also suitable for many biological events such as antigen-antibody interaction, protein-protein interaction, and the effects of changes in ion concentration. These unique capabilities of FCS enhance the opportunities to study dynamic molecular behavior, which is not possible with the other commonly used techniques. Furthermore, its potential will continue to be enhanced by technological advances in ancillary equipment such as CCD cameras and improved imaging modalities [28, 29].

On the other hand, the FCS target must have a fluorescent tag (e.g., GFP) and the size of the tag contributes to the observed signal in FCS. Therefore, much smaller fluorescent tags are needed. Recently, a tetracysteine tag, with only four to six amino acids, combined with biarsenical fluorophores was introduced as a new fluorescence labeling tool [30]. The small, 2-kDa tetracysteine tag should increase the accuracy of FCS signals. For the physical aspects of FCS, a narrower laser beam as well as a smaller optical volume would improve both the spatial and the temporal resolution of FCS. Furthermore, the capability of two-photon laser systems will reduce the background signal and increase the flexibility of sample preparation methods.

Conclusion

We have shown that the versatility of FCS in terms of sample preparation and sample analysis allows us to study new aspects of biological events. In this study of hERG, conventional biophysical and biochemical techniques such as patch clamping and immuno-staining would not have been able to reveal either the multiple protein populations during protein trafficking nor the distinct behaviors of the protein in the cytosol. We believe that FCS shows great potential to evaluate normal and abnormal protein trafficking in diseases such as cystic fibrosis, in which the mutant cystic fibrosis transmembrane conductance regulator (CFTR) Cl^- channel is abnormally folded and trafficked and is not functional at the plasma membrane [31]. FCS can also be applied to other genetic diseases to evaluate the effect and efficacy of drugs on the behavior of target proteins. For instance, it is now routine practice in the pharmaceutical industry to test compounds for hERG channel activity early in the drug-development process. We also expect that the application of FCS to the analysis of dynamic protein function will help to elucidate the mechanisms of some cardiac diseases, especially those involving abnormal protein trafficking that can be targeted for pharmacological treatment.

Acknowledgments We thank Dr. Masataka Kinjyo and the staff in his laboratory, Hokkaido University, for assisting us in establishing the FCS technique. We thank Drs. Bernardo Nadal-Ginard and Fuyuki Tokumasu for critical reading of the manuscript and for discussions regarding WT and G601S hERG. This work was supported by the Program for Promoting the Establishment of Strategic Research Centers, and Special Coordination Funds for Promoting Science and Technology from the Ministry of Education, Culture, Sports, Science and Technology of Japan.

References

1. Sanguinetti MC (1999) Dysfunction of delayed rectifier potassium channels in an inherited cardiac arrhythmia. Ann N Y Acad Sci 868:406–413
2. Furutani M, Trudeau MC, Hagiwara N, Seki A, Gong Q, Zhou Z, Imamura S, Nagashima H, Kasanuki H, Takao A, Momma K, January CT, Robertson GA, Matsuoka R (1999) Novel mechanism associated with an inherited cardiac arrhythmia: defective protein trafficking by the mutant HERG (G601S) potassium channel. Circulation 99:2290–2294
3. Anderson CL, Delisle BP, Anson BD, Kilby JA, Will ML, Tester DJ, Gong Q, Zhou Z, Ackerman MJ January CT (2006) Most LQT2 mutations reduce Kv11.1 (hERG) current by a class 2 (trafficking-deficient) mechanism. Circulation 113:365–373
4. Wilson AJ, Quinn KV, Graves FM, Bitner-Glindzicz M, Tinker A (2005) Abnormal KCNQ1 trafficking influences disease pathogenesis in hereditary long QT syndromes (LQT1). Cardiovasc Res 67:476–486
5. Akhavan A, Atanasiu R, Shrier A (2003) Identification of a COOH-terminal segment involved in maturation and stability of human ether-a-go-go-related gene potassium channels. J Biol Chem 278:40105–40112
6. Delisle BP, Anderson CL, Balijepalli RC, Anson BD, Kamp TJ, January CT (2003) Thapsigargin selectively rescues the trafficking defective LQT2 channels G601S and F805C. J Biol Chem 278:35749–35754
7. Kern A, Bryant-Greenwood GD (2009) Mechanisms of relaxin receptor (LGR7/RXFP1) expression and function. Ann N Y Acad Sci 1160:60–66
8. Brooks NL, Corey MJ, Schwalbe RA (2006) Characterization of *N*-glycosylation consensus sequences in the Kv3.1 channel. FEBS J 273:3287–3300
9. Li MS, Demsey AF, Qi J, Linsdell P (2009) Cysteine-independent inhibition of the CFTR chloride channel by the cysteine-reactive reagent sodium (2-sulphonatoethyl) methanethiosulphonate. Br J Pharmacol 157:1065–1071
10. Ficker E, Obejero-Paz CA, Zhao S, Brown AM (2002) The binding site for channel blockers that rescue misprocessed human long QT syndrome type 2 ether-a-gogo-related gene (HERG) mutations. J Biol Chem 277:4989–4998
11. Derler I, Hofbauer M, Kahr H, Fritsch R, Muik M, Kepplinger K, Hack ME, Moritz S, Schindl R, Groschner K, Romanin C (2006) Dynamic but not constitutive association of calmodulin with rat TRPV6 channels enables fine tuning of Ca_2+-dependent inactivation. J Physiol 577:31–44
12. Voss TC, Demarco IA, Day RN (2005) Quantitative imaging of protein interactions in the cell nucleus. Biotechniques 38:413–424
13. Cheezum MK, Walker WF, Guilford WH (2001) Quantitative comparison of algorithms for tracking single fluorescent particles. Biophys J 81:2378–2388
14. Qian H, Sheetz MP, Elson EL (1991) Single particle tracking. Analysis of diffusion and flow in two-dimensional systems. Biophys J 60:910–921
15. Magde D, Elson EL,Webb WW (1974) Fluorescence correlation spectroscopy. II. An experimental realization. Biopolymers 13:29–61
16. Kohl T, Haustein E, Schwille P (2005) Determining protease activity in vivo by fluorescence cross-correlation analysis. Biophys J 89:2770–2782
17. Rigler R (1995) Fluorescence correlations, single molecule detection and large number screening. Applications in biotechnology. J Biotechnol 41:177–186
18. Eigen M, Rigler R (1994) Sorting single molecules: application to diagnostics and evolutionary biotechnology. Proc Natl Acad Sci USA 91:5740–5747
19. Nomura Y, Tanaka H, Poellinger L, Higashino F, Kinjo M (2001) Monitoring of in vitro and in vivo translation of green fluorescent protein and its fusion proteins by fluorescence correlation spectroscopy. Cytometry 44:1–6

20. Vukojevic V, Pramanik A, Yakovleva T, Rigler R, Terenius L, Bakalkin G (2005) Study of molecular events in cells by fluorescence correlation spectroscopy. Cell Mol Life Sci 62:535–550
21. Yoshida N, Kinjo M, Tamura M (2001) Microenvironment of endosomal aqueous phase investigated by the mobility of microparticles using fluorescence correlation spectroscopy. Biochem Biophys Res Commun 280:312–318
22. Saito K, Ito E, Takakuwa Y, Tamura M, Kinjo M (2003) In situ observation of mobility and anchoring of PKCbetaI in plasma membrane. FEBS Lett 541:126–131
23. Martinez-Marmol R, Villalonga N, Sole L, Vicente R, Tamkun MM, Soler C, Felipe A (2008) Multiple Kv1.5 targeting to membrane surface microdomains. J Cell Physiol 217:667–673
24. Martens JR, Sakamoto N, Sullivan SA, Grobaski TD, Tamkun MM (2001) Isoform-specific localization of voltage-gated K+ channels to distinct lipid raft populations. Targeting of Kv1.5 to caveolae. J Biol Chem 276:8409–8414
25. Golebiewska U, Nyako M, Woturski W, Zaitseva I, McLaughlin S (2008) Diffusion coefficient of fluorescent phosphatidylinositol 4,5-bisphosphate in the plasma membrane of cells. Mol Biol Cell 19(4):1663–1669
26. Schmiedeberg L, Weisshart K, Diekmann S, Meyer Zu Hoerste G, Hemmerich P (2004) High- and low-mobility populations of HP1 in heterochromatin of mammalian cells. Mol Biol Cell 15:2819–2833
27. Murase K, Fujiwara T, Umemura Y, Suzuki K, Iino R, Yamashita H, Saito M, Murakoshi H, Ritchie K, Kusumi A (2004) Ultrafine membrane compartments for molecular diffusion as revealed by single molecule techniques. Biophys J 86:4075–4093
28. Ohsugi Y, Saito K, Tamura M, Kinjo M (2006) Lateral mobility of membrane-binding proteins in living cells measured by total internal reflection fluorescence correlation spectroscopy. Biophys J 91:3456–3464
29. Hassler K, Leutenegger M, Rigler P, Rao R, Rigler R, Gosch M, Lasser T (2005) Total internal reflection fluorescence correlation spectroscopy (TIR-FCS) with low background and high count-rate per molecule. Opt Express 13:7415–7423
30. Frischknecht F, Renaud O, Shorte SL (2006) Imaging today's infectious animalcules. Curr Opin Microbiol 9:297–306
31. Skach WR (2000) Defects in processing and trafficking of the cystic fibrosis transmembrane conductance regulator. Kidney Int 57:825–831